Title

INELASTIC ALPHA PARTICLE SCATTERING IN THE RARE EARTH REGION AND DETERMINATION OF

Authors

Hendrie, D.L.
Glendenning, N.K.
Harvey, B.G.
et al.

Publication Date

1967-06-01

UCRL-17547 Expanded

University of California

Ernest O. Lawrence Radiation Laboratory

DETERMINATION OF Y_4 DEFORMATIONS IN THE RARE EARTH REGION BY INELASTIC ALPHA PARTICLE SCATTERING

D. L. Hendrie, N. K. Glendenning, B. G. Harvey,
O. N. Jarvis, H. H. Duhm, J. Mahoney, and J. Saudinos

September 1967

DISCLAIMER

Submitted to the International Conference on
Nuclear Structure, Tokyo, September 7-13, 1967.

UCRL-17547 Expanded
Preprint

UNIVERSITY OF CALIFORNIA

Lawrence Radiation Laboratory
Berkeley, California

AEC Contract No. W-7405-eng-48

DETERMINATION OF Y_4 DEFORMATIONS IN THE RARE EARTH REGION BY INELASTIC ALPHA PARTICLE SCATTERING

D. L. Hendrie, N. K. Glendenning, B. G. Harvey, O. N. Jarvis
H. H. Duhm, J. Mahoney, and J. Saudinos

September 1967

DETERMINATION OF Y_4 DEFORMATIONS IN THE RARE EARTH REGION BY INELASTIC ALPHA PARTICLE SCATTERING

D. L. Hendrie, N. K. Glendenning, B. G. Harvey, O. N. Jarvis
H. H. Duhm, J. Mahoney, and J. Saudinos

Lawrence Radiation Laboratory, University of California, Berkeley, California

The study of alpha particle inelastic scattering has long been a fruitful method for investigation of collective nuclear excitation. The short wave length and large absorption of the alpha particles at the nuclear surface leads to distinct diffraction-type oscillations in the angular distributions in the forward hemisphere. The qualitative features of experimental results for states which are excited directly from the ground state are described by the Fraunhofer diffraction model(1) which provides a phase rule for location of maxima. More recently, experimental and theoretical results(2) have been obtained for states which cannot be directly excited. The angular distributions to these states contain features which distinctly mark them as proceeding through a cascade excitation mechanism, with diffraction phases opposite to the phase rule and less-steeply sloped angular distributions.

We have used the selective properties of medium-energy alpha scattering to perform a high-precision systematic investigation of the rare earth region of permanently-deformed nuclei. Our experiments consisted of scattering 50 MeV alpha particles from several isotopically-enriched metallic foils in the rare earth region. Scattered particles were detected in four moveable cooled lithium-drifted silicon detectors. Special care was taken to keep

---

[*] This work was done under the auspices of the U.S. Atomic Energy Commission.

backgrounds low and to achieve resolutions of about 50 keV. A sample spectrum is shown in Fig. 1. In Fig. 2 we see inelastic angular distributions for two of our target nuclei. The diffraction osciallations are evident and the

---

Captions to Figs. 1 and 2:

Fig. 1. Experimental spectra of two of the target nuclei, showing also some of higher excited states not included in the analysis.

Fig. 2. Angular distributions of excited rotational states of Sm^{154} and Yb^{176} excited 50 MeV alpha particles.

---

maxima in the 2^+ levels are located in accordance with the phase rule. However, higher levels differ in the two nuclei indicating differences in shape beyond Y_2.

The differential cross sections to the various members of the rotational band contain information relevant for the determination of the multipole expansion of the deformed nuclear field generated by the intrinsic ground state. Having measured the cross sections up to the 6^+ and sometimes 8^+ states, we are, therefore, in a position to determine the shape of the nuclear field up to Y_6. We shall parameterize the shape as illustrated in Fig. 3.

Caption to Fig. 3:

Fig. 3. Schematic view of permanently deformed nuclear shapes including positive and negative Y_{40} deformations.

Assuming that the alpha-nucleus interaction can be represented by a rigid deformed complex optical potential which describes the effects of the intrinsic excitations,(3) we have treated the rotation of the ground state explicitly by solving the complex coupled equations. Coulomb excitation effects were found to be important and were treated on equal footing with the nuclear excitation. The multipole expansion of the interaction, the number of coupled channels, and the number of partial waves were all carried to convergence, so that the calculation is an exact numerical solution of the scattering model.

Because we treat the rotations explicitly, the optical potential needs to take account of only the intrinsic excitations of the nucleus, and should, therefore, be essentially the same as for the nearby spherical nuclei.(3) We, therefore, determined these parameters from the elastic cross section of the spherical Sm^{148} nucleus and used them, with only very small adjustments, throughout the deformed region (see Table I). These parameters are of course very different than those obtained by treating only the elastic scattering on the deformed nuclei. This latter optical potential must implicitly account

Table I

	v	w	r	a	r_c
Sm^{148} elastic only	65.5	29.8	1.427	.671	1.40
Coupled-channels	65.9	27.3	1.440	.637	1.44
Sm^{154} elastic only	34.6	29.4	1.404	.819	1.40

for the effect of the rotations on the elastic cross section and because of the strong coupling, it is drastically modified as seen in Table I. It is the potential appropriate for a DWBA calculation of the cross section to the excited states. The results of such a calculation are shown in Fig. 4.

Caption for Fig. 4:

Fig. 4. Optical model and DWBA best fits to the scattering data on Sm^{154}.

The inability of the calculation to fit even the 2^+ state is apparent, and the DWBA approximation is clearly inapplicable.

A coupled-channels fit to the Sm^{154} data is shown in Fig. 5, using

---

Caption to Fig. 5:

Fig. 5. Coupled-channel calculation of 50 MeV alpha particles on Sm^{154} using β_2 and β_4 deformation of the nuclear shape. The theory and experiment agree in locations of maxima, slopes of the envelopes, magnitude of the cross sections, and depths of minima.

---

the optical parameters of Table I and adjusted deformation parameters β_2 and β_4. Notice that the experimental data are well-reproduced, even to relative depths of the minima of the various states. To indicate the sensitivity of the cross section to β_4, Fig. 6 shows results obtained by setting β_4 equal to zero

---

Caption to Fig. 6:

Fig. 6. Sensitivity of the cross sections of 50 MeV alpha particles to changes in the β_4 deformation parameters. The optical potential and β_2 were selected in each case to give a best fit to the 0^+ and 2^+ states.

---

and to negative 0.05. In both these cases the optical parameters and β_2 were readjusted for a best fit to the 0^+ and 2^+ states. We see in this way that the value of β_4 is quite accurately determined. The agreement found in Fig. 5 is somewhat improved by inclusion of a small β_6 as shown in Fig. 7. For almost

---

Caption to Fig. 7:

Fig. 7. Comparison of the experimental and coupled-channels results for Sm^{154} including a small negative β_6 term in the nucleus deformation.

---

all the nuclei we investigated, the agreement was somewhat improved by including a small negative β_6 term.

Fig. 8 shows the best fit to the data on Yb^{176}, again using the same

Caption to Fig. 8:

Fig. 8. Comparison of the experimental and best fit coupled-channels results for Yb^{176}. Notice that for this case a negative β_4 deformation term is needed to match the data.

optical parameters from Table I. In this case it was necessary to use a negative β_4. For comparison, the failure of the calculation to fit the data when the higher-order deformation terms are excluded is seen in Fig. 9. Fig. 10 shows the data and theory for Er^{166}; in this case we find no necessity for including a significant β_4 term, although the need for a β_6 term is most apparent here. Fig. 11 indicates the poor fit to the 6^+ level, when the β_6 term

Captions to Figs. 9 and 10:

Fig. 9. The deteriation of calculated fit to the upper levels of Yb^{176} when the higher-order deformation terms are excluded.

Fig. 10. Comparison of the experimental and coupled-channel results for Er^{166}. Although no β_4 term is necessary, the angular distribution to the 6^+ state indicates the need for a small negative β_6 term in the nuclear deformation.

Caption to Fig. 11:

Fig. 11. The poorer fit to the 6^+ level of Er^{166} when the β_6 deformation term is excluded.

is excluded. A summary of the results on the determination of the higher deformations is presented in Table II. The quadrupole moments of these shapes

Table II

Nuclide	Sm^{152}	Sm^{154}	Gd^{158}	Er^{166}	Yb^{174}	Yb^{176}	Hf^{178}
β_2	.205	.225	.235	.230	.230	.230	.205
β_4	.040	.045	.030	0	-.040	-.045	-.060
β_6	-.010	-.015	-.015	-.015	0	-.005	0
Q_o	6.42	7.15	7.76	7.95	8.24	8.23	7.55
$Q_o^{(a)}$	5.85	6.81	7.30	7.62	7.57	7.40	6.78

(a) Electric quadrupole moments calculated from the compilation of P. H. Stelson and L. Grodzins, Nuclear Data 1(1965), 21.

are also shown and compared to electric quadrupole moments. Of course they are not necessarily the same since our experiments determine the potential quadrupole moment.

In order to see whether or not these results for β_4 can be theoretically predicted, we have performed a calculation using a perturbation model developed by Harada for the actinide region. The model minimizes the binding energy of the nucleus using a Y_{40} deformation on the Nilsson potential and Nilsson wave functions. The results of the calculations are shown in Fig. 12 along with

---

Caption to Fig. 12:

Fig. 12. A theoretical calculation of β_4 in the rare earth region using the model of Harada, the experimentally determined values (adjusted for the difference between electromagnetic and optical radii) are also shown.

---

the measured values of β_4 obtained with the coupled-channels analysis. The calculation contains a somewhat arbitrary zero determination, corresponding to selection of contributing Nilsson orbitals. In comparison of the theory and experiment, the experimental β values were adjusted to account for the difference between electromagnetic and optical potential radii.

To summarize, we have measured with high precision the angular distributions of scattered alpha particles exciting members of the rotational band built on the ground state of even-even rare earth nuclei. The results were compared with a theory that solves the scattering problem exactly if one assumes that the interaction can be represented by an optical potential of rigid deformed shape. The detailed agreement between theory and experiment yields for the first time accurate measurements of higher-order deformations in these permanently deformed nuclei.

References

(1) J. S. Blair: Phys. Rev. 115(1959), 928.

(2) B. G. Harvey, D. L. Hendrie, O. N. Jarvis, J. Mahoney and J. Valentin: Phys. Letters 24B(1967), 43; N. Austen and J. S. Blair: Ann. Phys. 33(1965), 15.

(3) N. K. Glendenning: University of California Lawrence Radiation Laboratory Report, UCRL-17503 (1967), to be published in the Proceedings of the International School of Physics "Enrico Fermi," (1967), Academic Press.

(4) K. Harada: Phys. Letters 10(1964), 80.

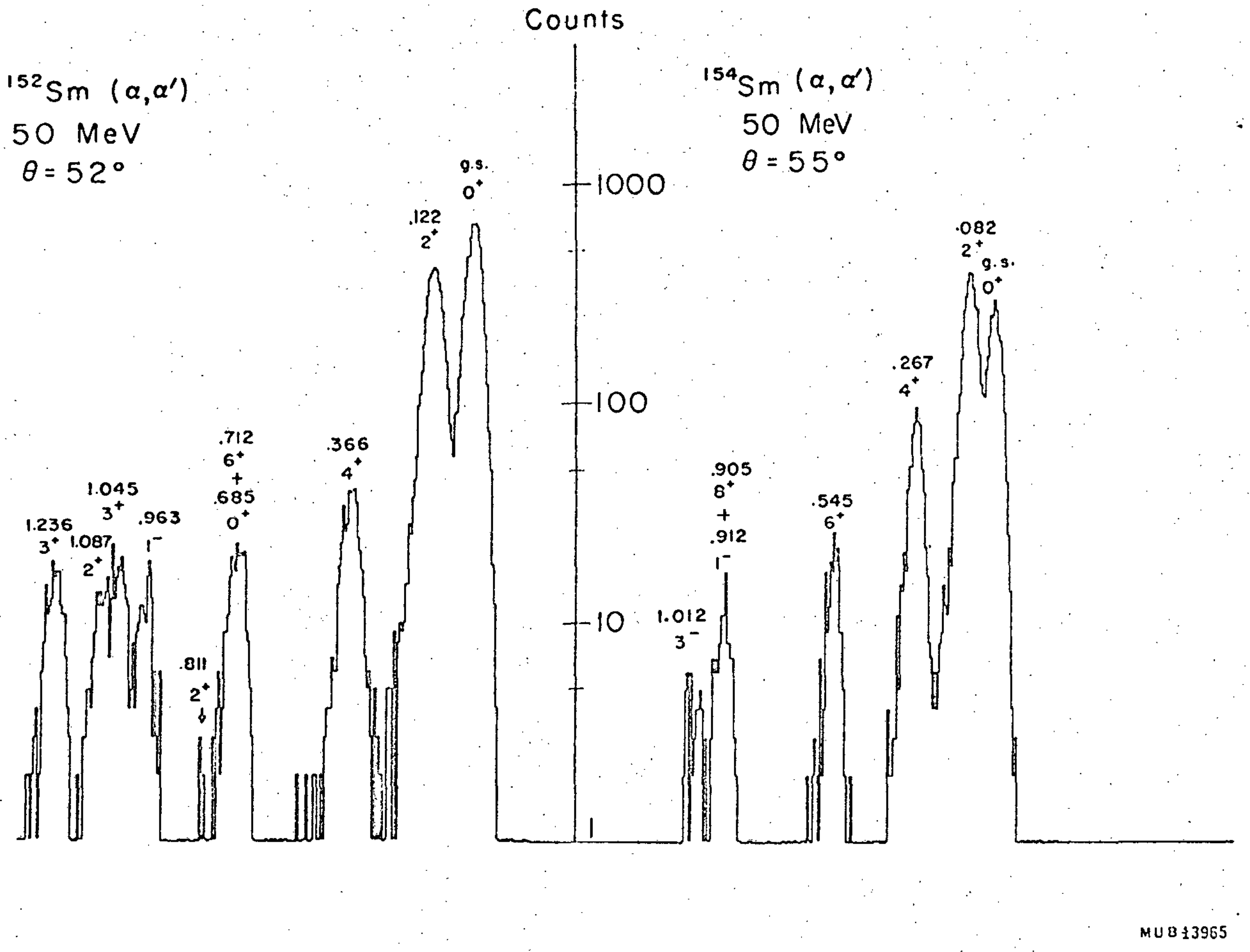
Counts
^{152}Sm (α,α′)
50 MeV
θ = 52°
^{154}Sm (α,α′)
50 MeV
θ = 55°
1000
100
10
1
g.s. 0+
.122 2+
.366 4+
.712 6+ + .685 0+
.811 2+
.963 1−
1.045 3+
1.087 2+
1.236 3+
.082 2+
g.s. 0+
.267 4+
.545 6+
.905 8+ + .912 1−
1.012 3−
MUB 13965

Fig. 1

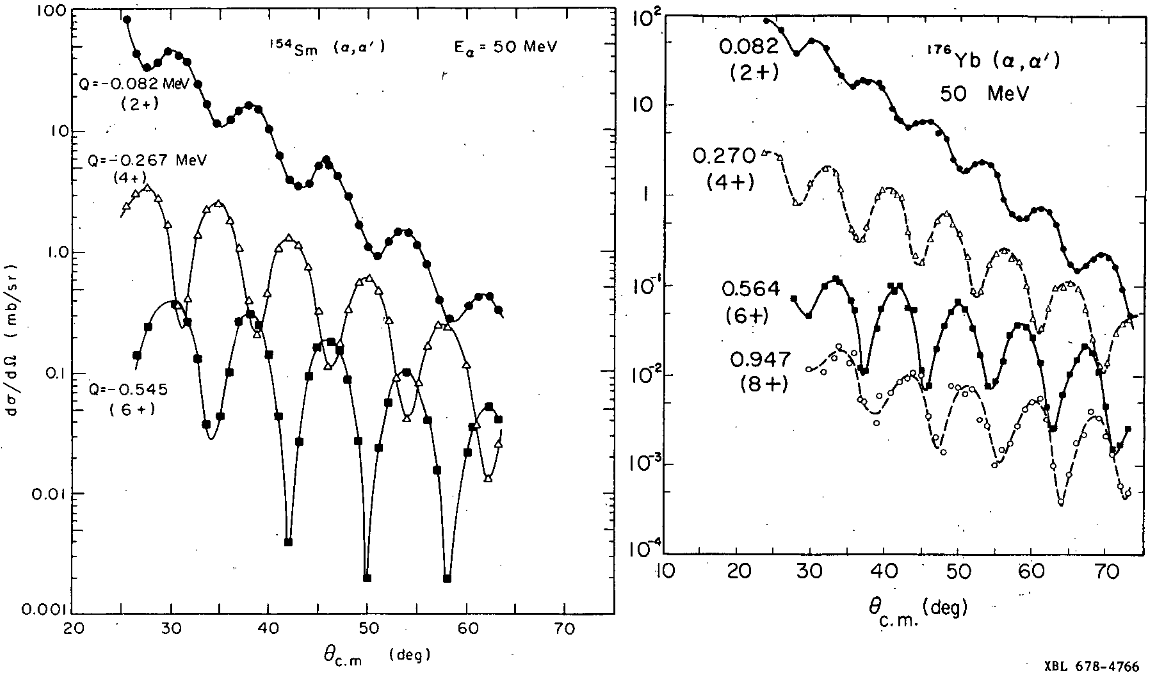

XBL 678-4766

Fig. 2

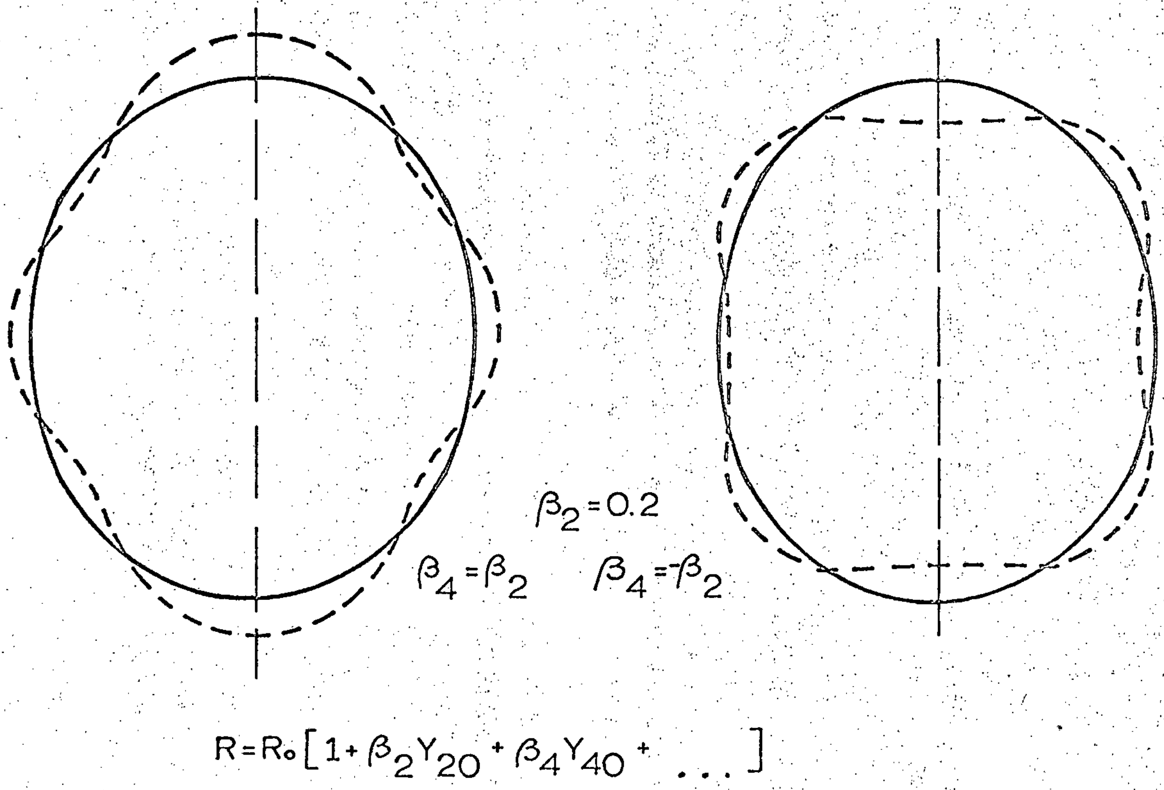

XBL 678-4765

Fig. 3

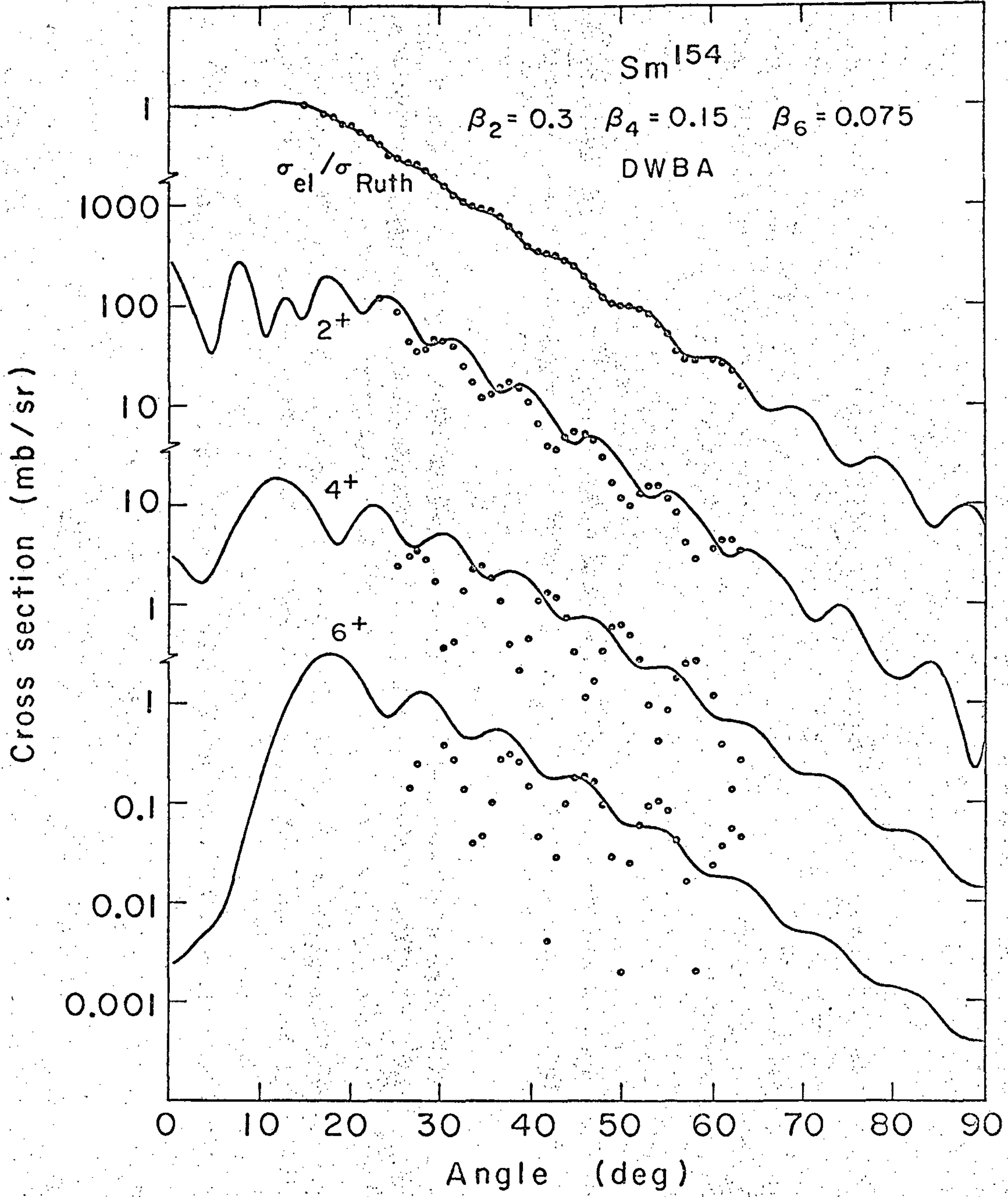

XBL677-3650

Fig. 4

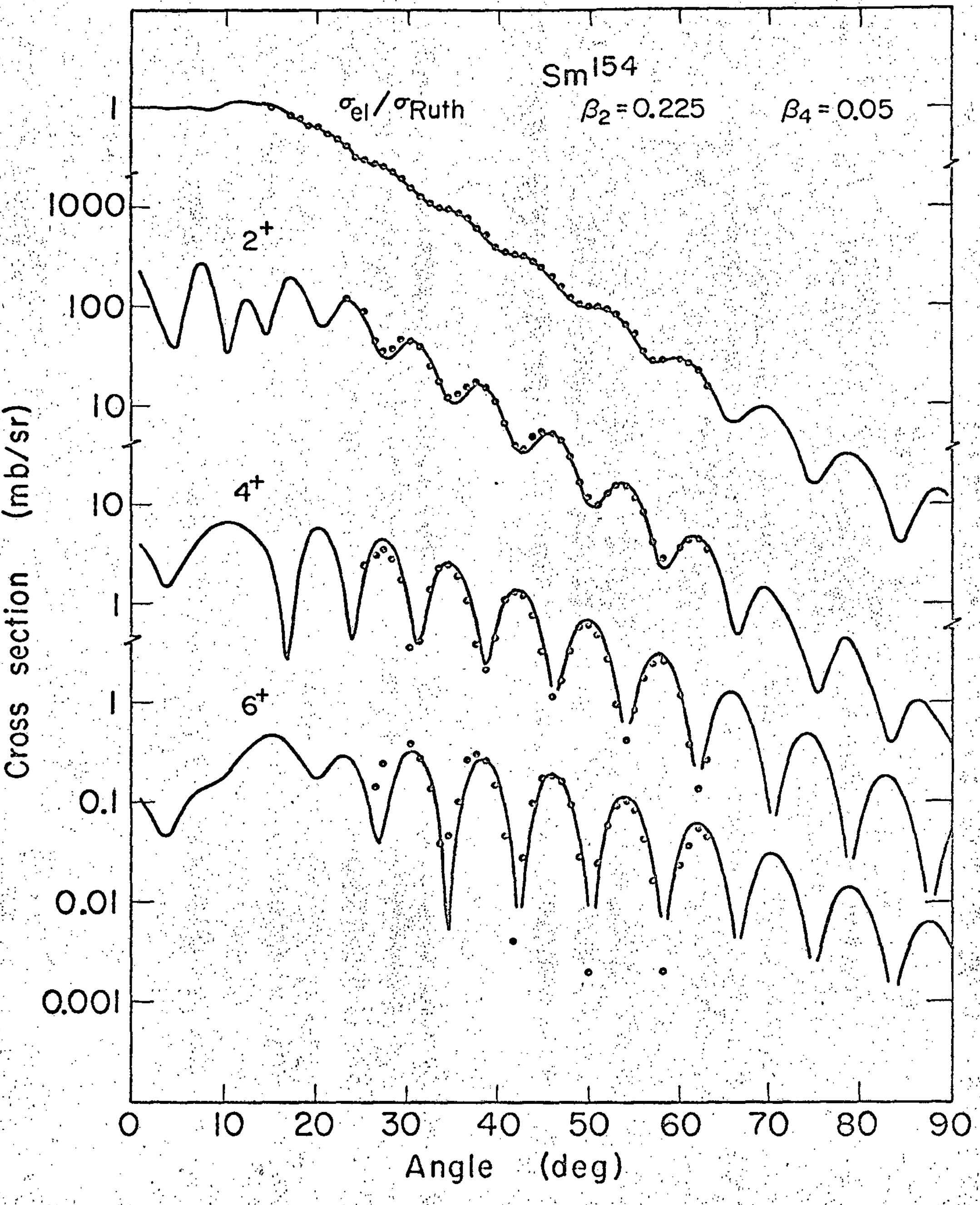
Sm154
σel/σRuth
β2 = 0.225
β4 = 0.05
2+
4+
6+
1
1000
100
10
10
1
1
0.1
0.01
0.001
Cross section (mb/sr)
0
10
20
30
40
50
60
70
80
90
Angle (deg)

XBL 677-3647

Fig. 5

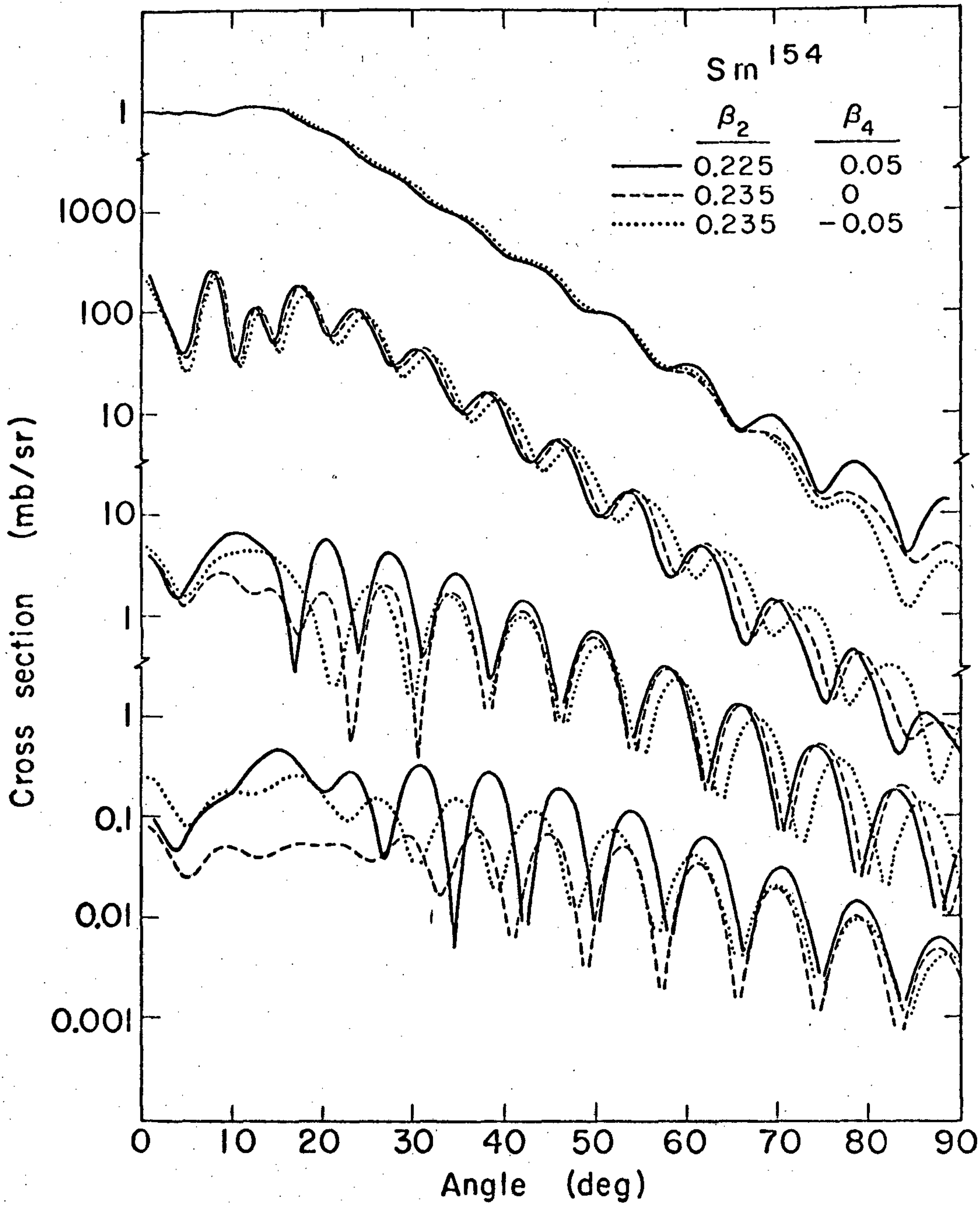

Sm^{154}
β_2 β_4
0.225 0.05
0.235 0
0.235 -0.05
1
1000
100
10
10
1
1
0.1
0.01
0.001
Cross section (mb/sr)
0 10 20 30 40 50 60 70 80 90
Angle (deg)
XBL677-3652

Fig. 6

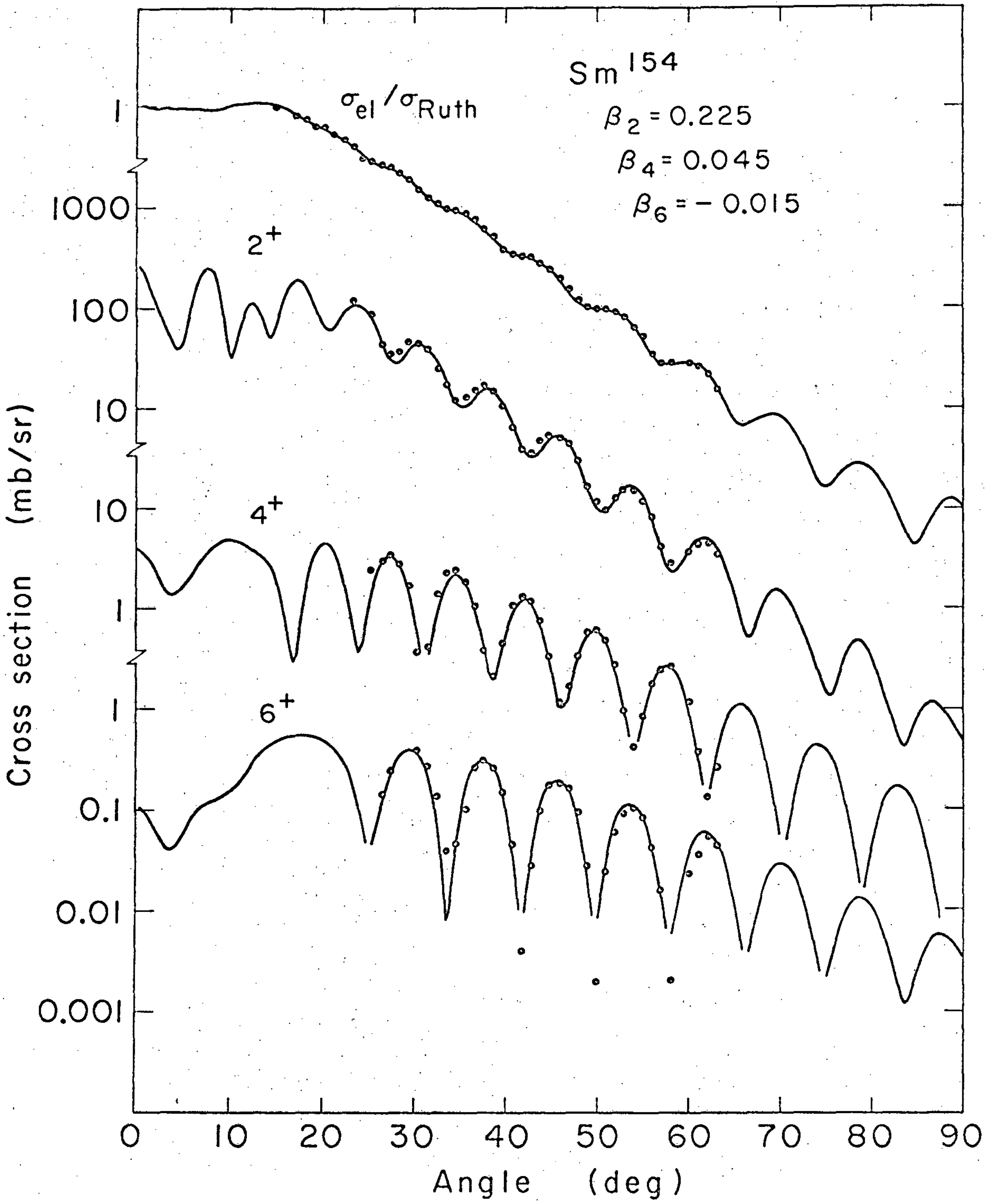

XBL678-3849

Fig. 7

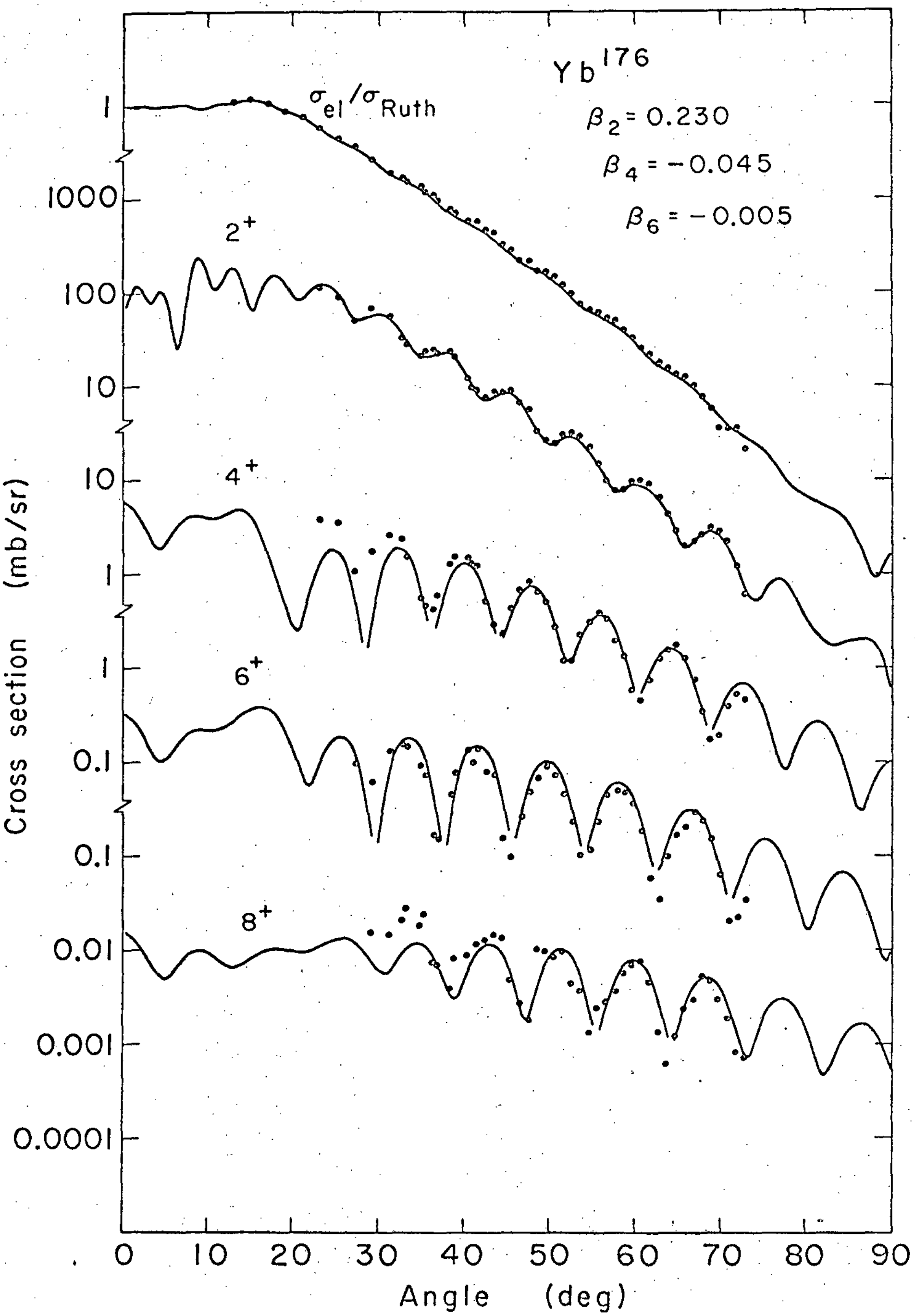
Yb^{176}
β_2 = 0.230
β_4 = −0.045
β_6 = −0.005
$\sigma_{el}/\sigma_{Ruth}$
2^+
4^+
6^+
8^+
1
1000
100
10
10
1
1
0.1
0.1
0.01
0.001
0.0001
Cross section (mb/sr)
0
10
20
30
40
50
60
70
80
90
Angle (deg)
XBL678-3853

Fig. 8

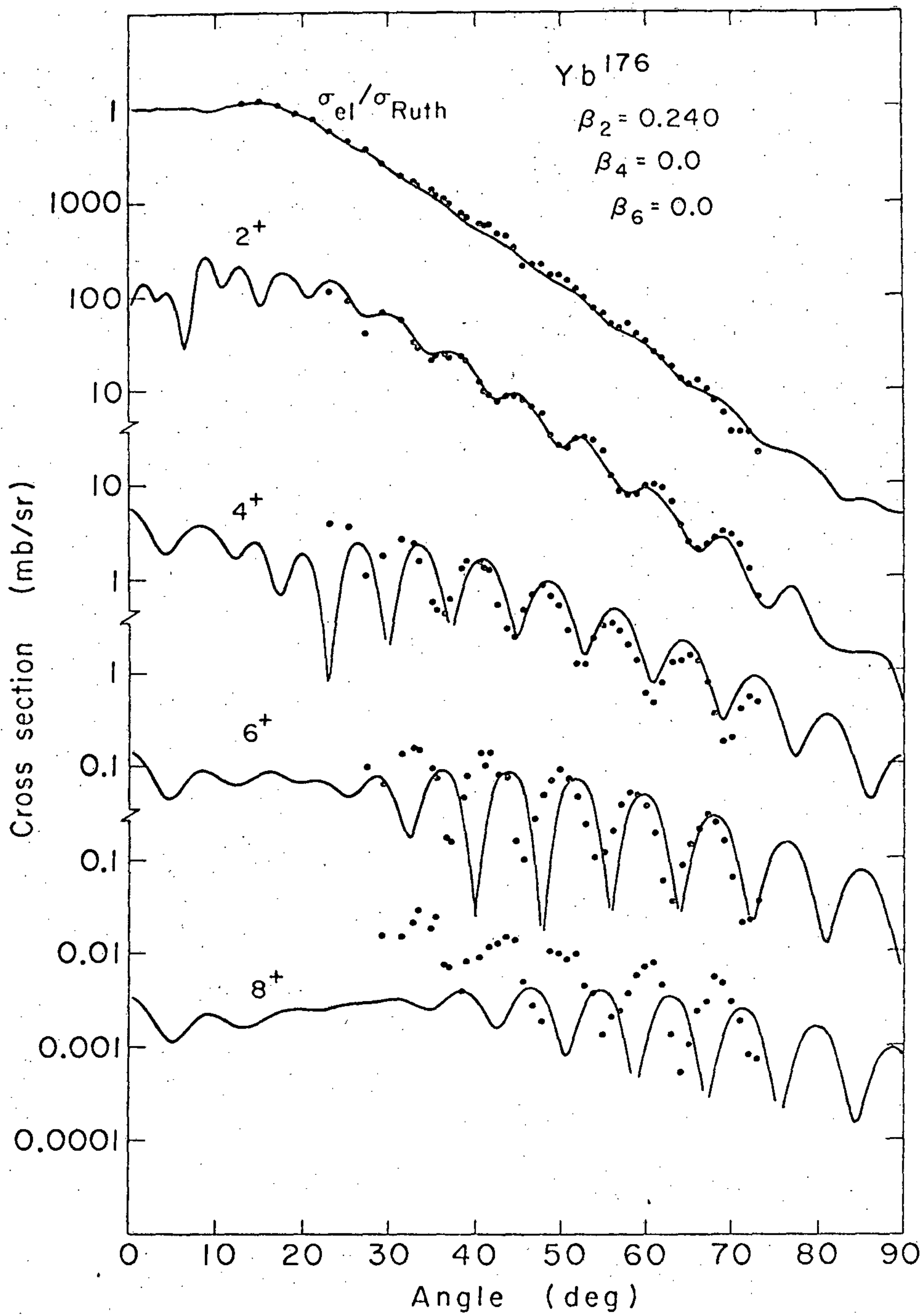
Yb176
β_2 = 0.240
β_4 = 0.0
β_6 = 0.0
$\sigma_{el}/\sigma_{Ruth}$
2+
4+
6+
8+
1
1000
100
10
10
1
1
0.1
0.1
0.01
0.001
0.0001
Cross section (mb/sr)
0
10
20
30
40
50
60
70
80
90
Angle (deg)
XBL678-3852

Fig. 9

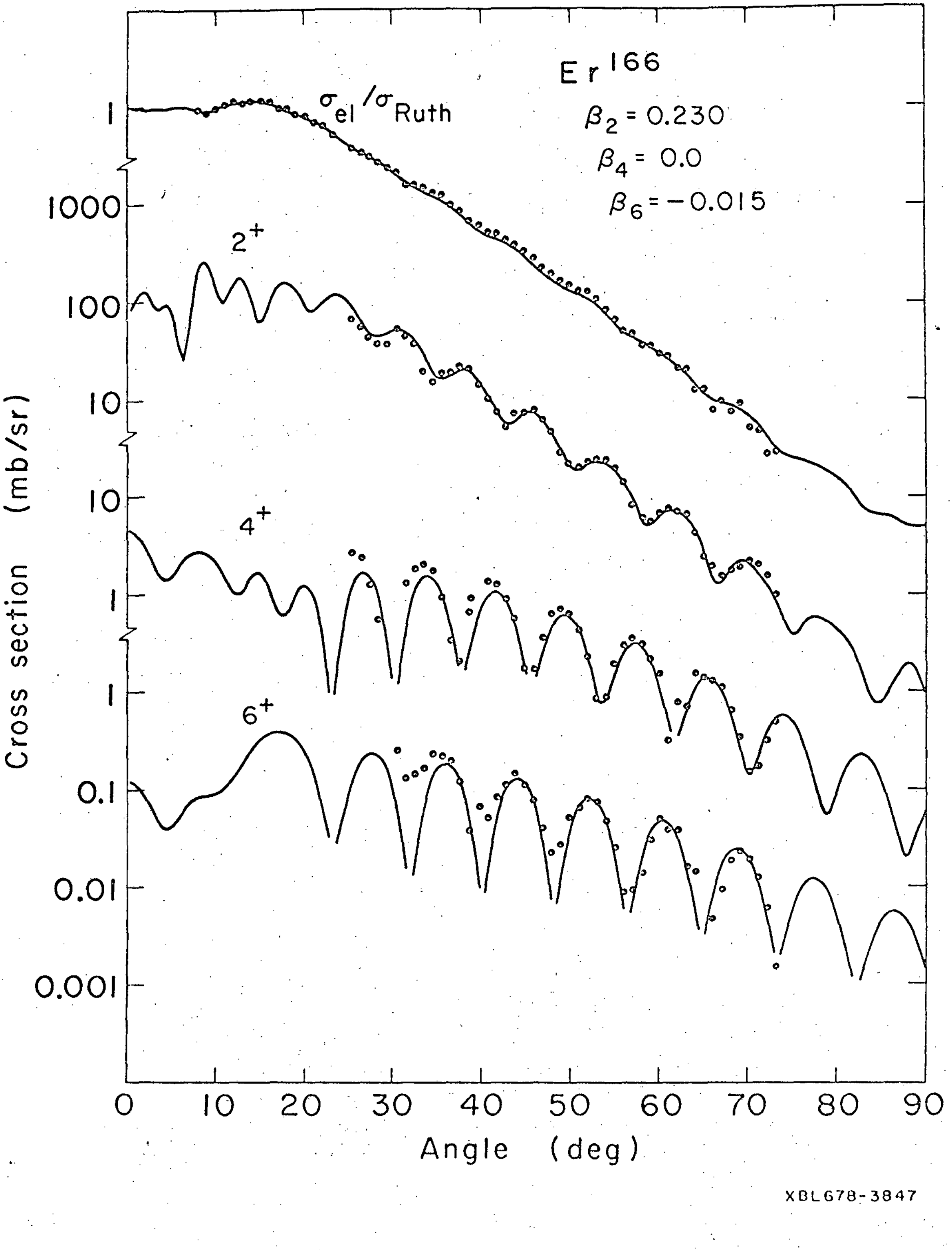

XBL678-3847

Fig. 10

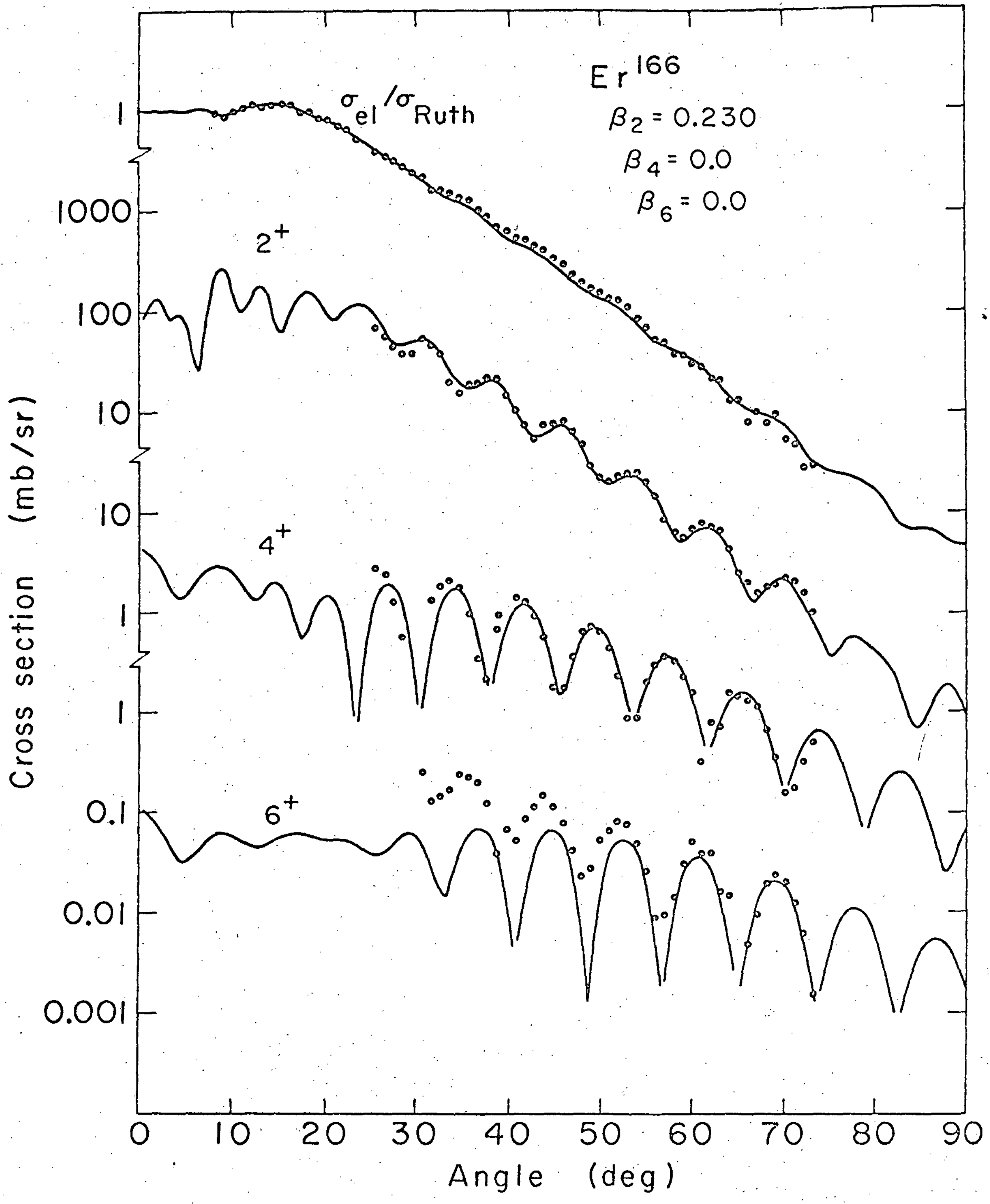

XBL678-3846

Fig. 11

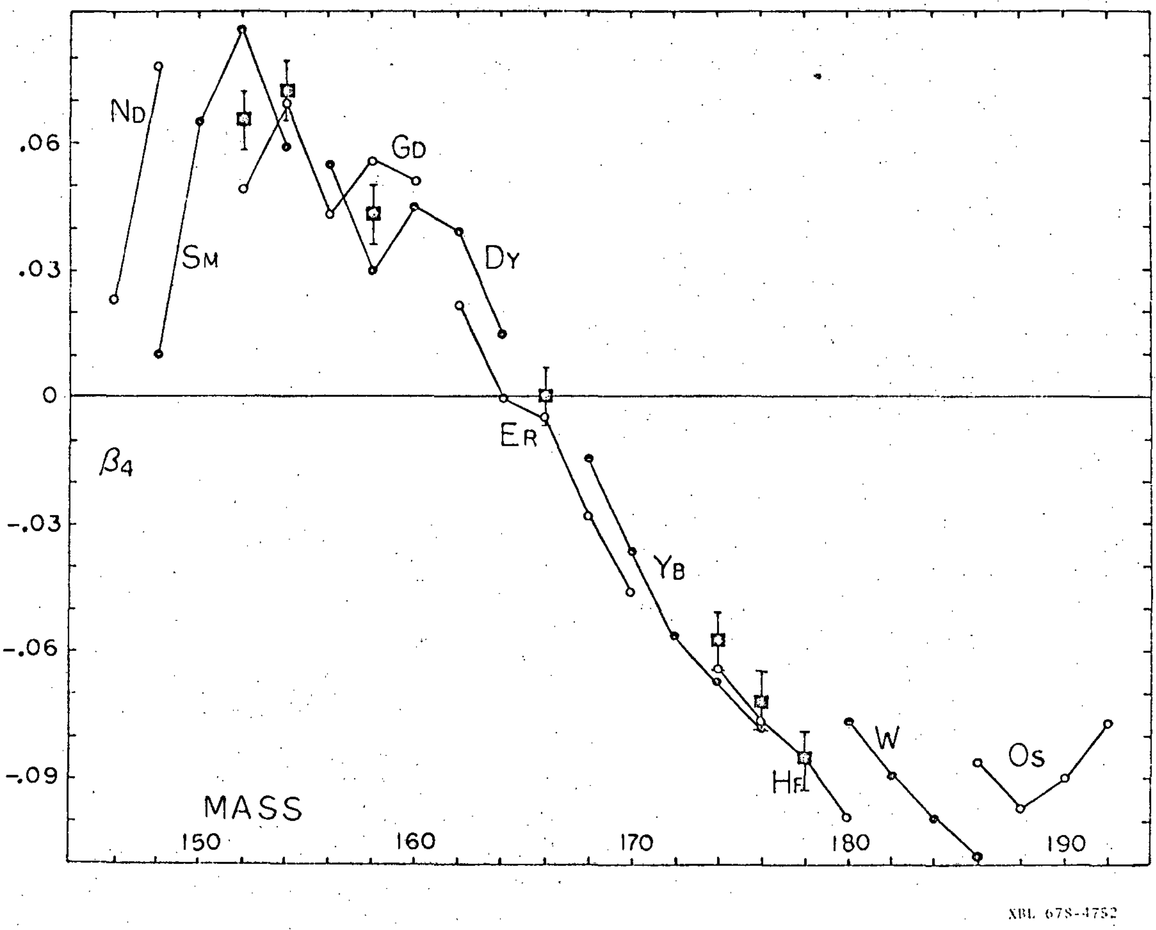
ND
SM
GD
DY
ER
YB
HF
W
OS
.06
.03
0
-.03
-.06
-.09
β4
MASS
150
160
170
180
190
XBL 678-4752

Fig. 12